COMPUTATIONAL STUDY OF CANARY GREENHOUSE SIDE WALL AND ROOF VENTS OPENING EFFECT ON NOCTURNAL AIRFLOW AND CLIMATE PATTERNS

Hassan Majdoubi[1,3*], Hicham Fatnassi[2], Thierry Boulard[2], Allal Senhaji[3], Salma Elbahi[1], Hassan Demrati[4], M'hamed Mouqallid[3], Lahcen Bouirden[4]

ABSTRACT

The following paper presents a Computational Fluid Dynamic (CFD) comparative study of the effect of side wall and roofs vents openings on canary greenhouse airflow circulation and climate distribution under different ventilation processes. The investigation was conducted in a one hectare canary greenhouse type, which is the most widespread type in the whole Mediterranean and along the Atlantic coast area of Morocco, especially in souss vally region. The simulations were performed with the commercial code CFD2000 based on the solution of the partial differential equations, which describe the flows, and was obtained by discretizing the space and time and solving the transport equations on the spatial grid as difference equations, used a finite volume discretization. The standard two equations k-ε model was used to describe the turbulent transport. The influence of external factors such the cover temperature, the wind speed, on the flow was simulated by boundary conditions, these values were obtained from experimental results. Simulations were conducted with a fixed wind speed equal 1.05 m/sec, tomato crop rows oriented north-south and the ventilation openings are continuous and equipped with insects screen type 20/10. Results reveal that ventilation opening arrangements strongly affects the greenhouse wind speed, which can generate a heterogeneous climate, especially during daytime. But in the other hand, results confirm that there is no significant effect of the side wall vents opening on canary greenhouse air temperature and humidity fields.

Key words: Greenhouse, CFD, Insect screen, Ventilation openings, Climate

[1]Laboratoire de Recherche Scientifique et Pédagogique au Monde Méditerranéen, CRMEF Meknès-Tafilalet, Meknès, Maroc, majdoubi76@yahoo.fr

[2]INRA, Univ. Nice Sophia Antipolis, CNRS, UMR 1355-7254 Institut Sophia Agrobiotech, 06900 Sophia Antipolis, France

[3]Equipe de recherche en Energétique et Mécanique des Fluides, ENSAM Meknès, Maroc

[4]Laboratoire de Thermodynamique et Energétique (LTE), Faculté des Sciences, Agadir, Maroc

**Corresponding Author*

INTRODUCTION

Greenhouse production technology systems, no matter where, consist of fundamental climate control components, and depending on their design and complexity, they can provide a greater or lesser amount of climate control, and subsequent plant growth and productivity. Temperature and humidity are the most important parameters of the greenhouse climate that needs to be controlled in order to achieve optimal plant growth and maximize the yield. During day time especially in hot climate conditions, the major concern for greenhouse climate management is to extract the excess energy. This can be obtained by removing the extra heat through air exchange by means of ventilation openings. Contrarily, by night, especially in cold climate conditions, the challenge for greenhouse growers is to keep the heat received during the day in order to have a higher inside temperature than outside. This can be realized by using an internal curtain and/ or closed the ventilations openings.

Natural ventilation is most important for controlling the temperature and humidity level. Several studies were been conducted on ventilation rate effect on airflow and microclimate distribution. Feuilloley et al., 1994, suggested a simple and efficient way for a grower or constructor to determine the dimension of the vents of natural ventilation for tunnel greenhouses in Mediterranean climate. Boulard et al., (1995 a & b), have studied by measurements the air exchange rate of a twin-span plastic greenhouse with continuous roof vents and by simulation. Kittas et al., (1995 & 1996), studied again the ventilation in the same greenhouse as Boulard et al., (1995) presented a non-dimensional ventilation function per unit of greenhouse window and ground areas, respectively. Sase et al., (2006), have analyzed the air movement and their effect on microclimate uniformity in a single span ventilated greenhouse. They show that the internal air movement in a naturally-ventilated greenhouse is affected by many factors such as wind velocity, wind direction, temperature difference between internal and external air, greenhouse structure and vent configuration that includes size, shape and arrangement of vent openings. Also Willits (2006) examined the effect of airflow rate, outside relative humidity, and canopy size on the behavior of the evapotranspiration coefficient and upon thermal stratification.

Fatnassi et al., (2009), experimental study confirmed the dependence of the greenhouse tunnel ventilation on wind direction and crop status, results show that the air exchange rate of a tunnel type greenhouse decreases with crop height, the high leaf density near the ventilation opening area causing an additional air pressure drop. More Recently, the coupled approach between energy balance simulations and computational fluid dynamics was used by Piscia et al., (2015), in order to analyze the effects of ventilation on greenhouse climate under different sky climate conditions, the study's results indicate that ventilation during the night-time, in winter time, improves greenhouse climate; in the clear-sky case, relative humidity was reduced and the temperature was raised since ventilation reduced or eliminated thermal inversion, whereas in the covered-sky situation, ventilating reduced the humidity content, but the temperature dropped.

Canary and Spanish 'Parral' greenhouse are naturally ventilated through the combination of sidewalls, operated manually, and opened fixed roof ventilators openings. Unfortunately, up to now, very few studies were conducted on canary greenhouse ventilation openings effect on airflow and microclimate distribution. Demrati et al., (2007), have used the energy balance method to predict the greenhouse ventilation rate of a banana crop canary greenhouse. Some authors used computer programs to investigate the influence of insect screens and predict the inside microclimate distribution, Fatnassi et al., (2003 & 2006) have characterized the inside climate distribution and the air exchange rate of 0.5 ha canary type greenhouse, equipped with insect screens (6×6) on side and roof ventilation openings, then used these data for the validation of a three dimensional CFD simulation model. Campen (2003) and Molina-Aiz (2004) have analyzed the effect of wind speed and direction and the ventilation openings design on natural ventilation of a Spanish 'Parral' greenhouse equipped with screened top and side ventilation. Result obtained by Majdoubi et al., (2007), showed that the relatively "bad" ventilation performance of canary greenhouse is not a result of the low value of the greenhouse wind‒related ventilation efficiency coefficient (Cw) but a result of the low value of the discharge coefficient (Cd), caused by a high pressure drop along the air circulation. This latter is generated both by the use of fine insect screens with small openings and obstruction due to the crop rows orientation which was perpendicular to the prevailing wind direction.

As a previous CFD study, Majdoubi et al., (2009), have analyzed the air circulation and the distributed climate during daytime in a 1-ha Canary type tomato greenhouse in the coastal area of southern Morocco. Analyses show that even with low outside wind speed, the outside wind governs the inside airflow, inducing a strong wind wise air current above the canopy and a very slow reverse flow inside the crop canopy. The weak air exchange within the canopy governs the climate at this level, with a major increase in air temperature and a more moderate increase in specific humidity. Keeping in mind these researches, in this paper, was designed a 3D CFD model to investigate the effect of different ventilation openings configurations on canary greenhouse climate during night time. Simulation conducted in the same greenhouse already studied by Majdoubi et al., (2009) by using a commercial CFD package (CFD2000®/ Storm), the airflow circulation, temperature and humidity fields within a real large scale Moroccan canary greenhouse (1.125 ha area) equipped with insect screens (20/10) on the roof and sidewalls ventilation openings. A realistic model based on energy, mass and momentum exchanges was considered. As the regime in greenhouse is turbulent, the turbulent transfers were described by a k-ε model. Likewise, the dynamic influences of insect screens and tomato crop on airflow movement were modeled by means of the concept of porous medium with the Boussinesq assumption. Atmospheric radiations contribution was included in the model by customizing the roof cover temperature deducted from its energy balance by means of view factor law. Also, the CFD code was customized in order to simulate, in each element of the crop cover, the sensible and latent heat exchanges between tomato crop and greenhouse.

The CFD Model

i. Fluid flow equation

The velocity field U, and the associated temperature field T or water vapor content w can be deduced at any time from the resolution of the mass, momentum and energy balances:

$$\frac{\partial \Phi}{\partial \tau} + \sum_{j=1} \frac{\partial}{\partial X_j}(U_j \Phi) = \sum_{j=1} \frac{\partial}{\partial X_j}(\Gamma_\Phi \frac{\partial \Phi}{\partial X_j}) + S_\Phi \tag{1}$$

Where Φ is the studied variable, either the three components of the speed vector, the temperature T or a given mass component such as the air humidity content w, Γ_Φ is the diffusion coefficient of the quantity Φ, S_Φ the source term and U_j the speed component. The governing equations are discretized following the procedure descripted by Patankar (1980). This consists of integrating the governing equations over a control volume. Theses equations are numerically solved using a finite volume code CFD2000 using the PISO algorithm developed by Issa (1985) (CFD2000® manual, 2004). This code also allows for the modeling of the turbulent constraints by means of the standard k-ε turbulence model (Launder, 1974).

ii. Flow through a porous medium

In order to include the drag effect inducted by the insect screens and the crop cover, into our CFD study, the insect screens and the crop cover were simulated as porous medium and the air flows governed by the Darcy-Forchheimer equation (2):

$$S_{\Phi} = -((\mu/K)U + \left(C_F/\sqrt{K}\right)U^2) \quad (2)$$

Where U is the air speed, µ is the dynamic viscosity of the fluid, K is the permeability of the porous medium and is the non-linear momentum loss coefficient. The values of the aerodynamic proprieties (K and CF) of the porous medium (screen) were calculated using relations from literature, which correlate these proprieties with the porosity (Miguel, 1997)

$$K = 3{,}44\ 10^{-9}\alpha^{1,6} \quad (3)$$

$$C_F = 4{,}30\ 10^{-2}/\alpha^{2,13} \quad (4)$$

Where α is screen porosity, it can be deduced from the dimensions of the thread [21]:

$$\alpha = L.l/\left((L+d)(l+d)\right) \quad (5)$$

Where L = 0.788 mm and ℓ = 0.255 mm are mesh's length and width respectively, and d = 0.28 mm, is the wire diameter.

For the crop, this sink of momentum is proportional to the leaf density and it may be expressed by unit volume of the cover by the commonly used formula (Bruse, 1998):

$$S_{\Phi} = -LAI\ C_D U^2 \quad (6)$$

Where LAI is the leaf area index and CD is the drag coefficient of the vegetal cover. For a mature greenhouse tomato crop, Haxaire (1999) found $C_D = 0.32$, using wind tunnel facilities.

For the crop and the range of air speed observed into the cover, the term in U of equation (2) can be neglected in front of the quadratic term and the non-linear momentum loss coefficient CF and the permeability K of the medium can be deduced from the combination of equations (2) and (6):

$$C_F/\sqrt{K} = LAI\ C_D \quad (7)$$

For our simulations, the tomato crop cover was assimilated to a unique 2.6 m high parallelepiped block of porous medium with the same length and width than the greenhouse and with a leaf area index, LAI, equal to 3, the drag coefficient CD being equal to 0.32 (Haxaire, 1999)

iii. Simulation of dynamic, thermal and hydrous effects of the crop cover

The coupled sensible and latent heat balances were considered at crop level by means of the equations describing respectively the sensible and the latent exchange, within each mesh of the crop assimilated to a porous medium, between the greenhouse air and the solid matrix of the porous medium. The radiative flux, reaching each mesh of the crop cover was assimilated to a "volumic heat source boundary condition" and partitioned into convective sensible and latent heat flux (water vapor) depending on the heat and water exchanges between air and the virtual solid matrix representing the crop cover and characterized by its surface temperature:

$$R_{net} + Q_{sens} + Q_{lat} = 0 \quad (8)$$

The sensible heat flux Q_{Sen} can be expressed with respect to the difference of temperature between inside air and the canopy:

$$Q_{Sen} = \rho C_p LAI\left((T_v - T_i)/r_a\right) \quad (9)$$

and the latent heat flux Q_{Lat} deduced from a similar relation :

$$Q_{Lat} = \rho L_v L_e^{\frac{1}{3}} LAI\left((w*_v - w_i)/(r_a + r_s)\right) \quad (10)$$

Where C_p and ρ are respectively the specific heat of air at constant pressure (J kg^{-1} K^{-1}) and the air density (kg m^{-3}), T_i is the greenhouse air temperature (K), T_v is the vegetation temperature (K), r_a the aerodynamic resistance between the leaf and the air within each mesh (s m^{-1}), L_v is the latent heat of vaporisation of water (J kg^{-1}), w_v^* is the saturated water content of the air at vegetation temperature (kg kg^{-1}), w_i is the air water vapor content (kg kg^{-1}), r_s is the leaf stomatal resistance (s m^{-1}) and L_e the Lewis number.

In order to take into account these new exchanges, the CFD code was customized by means of a "source model" (Haxaire, 1999):

$$Source = Coef.(value - Dependent \quad variable) \quad (11)$$

Where the different terms of this equation were identified with the terms of the sensible and latent heat transfer equations between the crop cover and the air within each mesh, i.e. for the temperature :

$$Coef = LAI\rho Cp/r_a \text{ and } value = T_v \ ,$$

and for air humidity:

$$Coef = LAI.\rho.L_v.L_e^{\frac{1}{3}}/r_a + r_s \text{ and } value = w_v .$$

The aerodynamic resistance r_a was deduced from the air speed within each mesh:

$$r_a = \rho C_p / 0.288\lambda \left(d_v \nu / \left\| \vec{U} \right\| \right)^{0.5} \qquad (12)$$

Where d_v is the characteristic length of the leaf (m), U_i the interior air speed (m s-1), λ is the air thermal conductivity (W m^{-1} K^{-1}) and ν is the air viscosity.

The radiative flux was considered as not limiting and the tomato leaf stomatal resistance deduced from air temperature and saturation deficit (Boulard et al., 1991):

$$r_s = r_{s_{\min}} \left\{ 1 + 0.11 \exp \left[0.34 (6.107\, 10^{\frac{7.5 T_i}{237.5 + T_i}} - 1629 w_i - D_{\max}) \right] \right\} \qquad (13)$$

Where: $r_{s_{\min}} = 150\ s\ m^{-1}$ et $D_{\max} = 10\ mbar$

Tomato crop temperature and humidity can be customized and calculated in simulation model according to the following equations (Majdoubi et al., 2009):

$$T_f = T_{\text{int}} + \frac{r_a}{\rho . C_p} \left[\frac{1}{2LAI_v} \left(\frac{dR(z)}{dz} - \rho . L_v \frac{w_{\text{int}} - w_a}{r_t} Lai_v \right) \right] \qquad (14)$$

$$\frac{\rho}{r_s}(w_{\text{int}} - w_f) = \frac{\rho}{r_a}(w_f - w_a) \quad or \quad w_f = \left(\frac{w_{\text{int}}}{r_s} + \frac{w_a}{r_a} \right) / \left(\frac{1}{r_a} + \frac{1}{r_s} \right) \qquad (15)$$

with LAI is the crop stand leaf area index and R(z) is the global radiation inside the greenhouse

v. Meshes and boundary conditions

The computational grid used Cartesian body fitted coordinates and after several trials with different densities, the calculations were based on a 192 by 44 by 112 grid with finer resolutions were imposed near soil, walls and roof, due to stronger thermal gradients (Figure 1) (Majdoubi et al., 2009). The boundary conditions prescribed a null pressure gradient in the air, at the limit of the computational domain. The outside air speed was perpendicular to the West–East sidewalls ventilation openings with a measured value equal 1.05 ms^{-1}. The driving force of natural convection is the wind force and buoyancy force arising from small temperature differences within the flow according to the boussinesq hypothesis. The averages and standard deviations of the climate boundary conditions are summarized in Table 1.

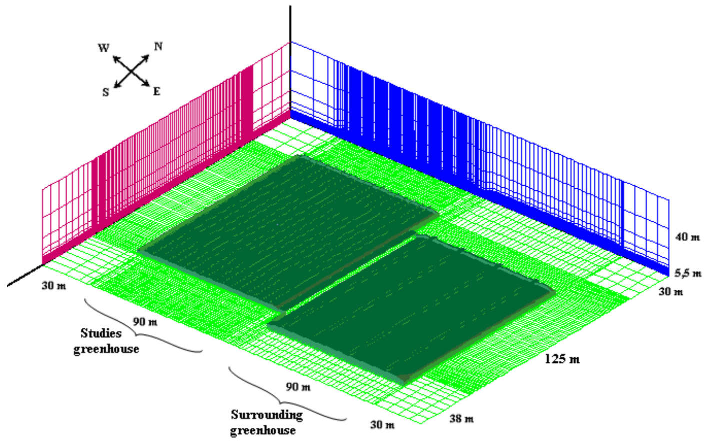

Figure 1.Computational grid of the whole domain for the CFD simulation (Greenhouse, tomato crop and insect screens)

Table 1. Experimental measurement (mean and S.D) performed between 2 and 5 h (end of night) during 3 days during summer time and used as boundary conditions for the simulation

Parameters	Mean	S.D
Outside temperature T_e (°C)	18.67	1.05
Outside relative humidity HR_e (%)	91.49	3.6
Sky temperature T_{sky}(°C)	6.23	0.75
Crop cover temperature T_v (°C)	18.11	1.23
Soil surface temperature T_{si} (°C)	20.34	0.98
Wind direction D v (degré)	120.11	10.45
Wind speed U (m/s)	1.05	0.023
Solar radiation (W/m^2)	0	0
Net radiation R_{net} (W/m^2)	-9.15	0.53
Inside soil surface flux Fs (W/m^2)	-15	1.21

MATERIALS AND METHODS

i. Site and greenhouse description

The experimental greenhouse is a large scale commercial canary plastic greenhouse covered with a 200 µm thickness single layer polyethylene plastic. Its surface occupies 1.125 ha (90 m length and 125 m width) with a height of 5 m at the gutter and 5.5 m at the ridge and was surrounded by similar greenhouses. The orientation of its spans and tomato crop rows was North-South, i.e, perpendicular to the direction of the prevailing sea wind.

Greenhouse ventilation was performed by means of seventeen roof ventilation openings (0.6×125 m^2 each, total of 1.275 m^2) covered with insect screens (20 meshes.cm^{-1} in width, 10 meshes.cm^{-1} in length with a wire diameter of 0.28 mm). The sidewalls ventilation openings were equipped with similar insect screens. The maximal opening areas reached 875 m² for the West-East sides and 630 m^2 for the North-South sides. During the experiment, the roof and sidewalls openings were maintained unchanged and equal to 1,275 m^2 and 1,505 m^2 respectively (Figure 2).

The greenhouse was occupied by a tomato crop (Solanum Lycopersicum, cv. Gabriella) planted with a plant density of 1.8 plant m^{-2} and north-south oriented rows, i.e. perpendicular to the prevailing see breeze direction coming from west.

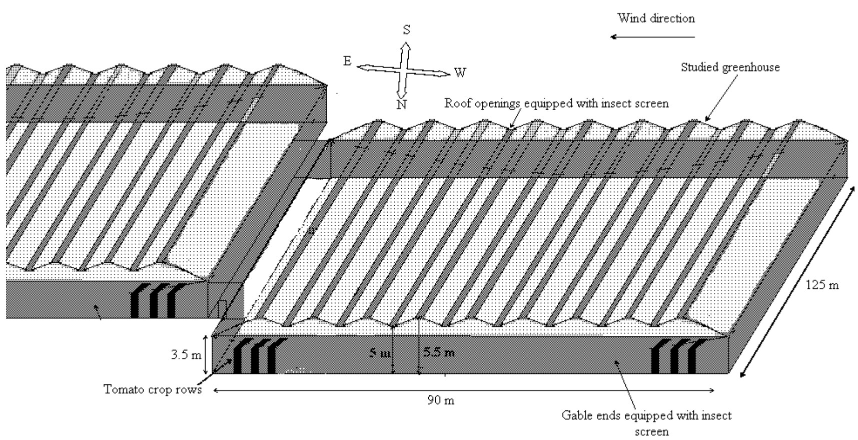

Figure 2. Schematic view of the studied greenhouse, its ventilation system and the surrounding.

ii. Inside and outside climatic parameters measurements

The following parameters were systematically recorded:

- The inside net radiation Rnet was monitored by means a net radiometer (Q-7, Campbell Scientific Ltd, UK), situated between the top of the crop canopy and the polyethylene film of the roof.
- The inside conductive heat flux exchange at soil surface FS which was measured by means of a conductive flux meter (HFT3, Campbell Scientific Ltd, UK) situated 1 mm below the soil surface.

- The inside and outside air temperature T and relative humidity HR were measured by means of thermo-hygrometers probes (HMP45 AC, Vaisala, Etoile Internationale, Paris)
- The inside soil surface, roof cover, tomato leaf temperatures were measured by means of thermocouples (Copper- Constantan) which were stuck on the plastic or positioned 1mm below the soil surface together with fine thermocouples which were inserted in the principal vein of the terminal leaflet on the lower face of a leaf.
- The outside wind speed U and direction Dv were measured by means of a cup anemometer and a wind vane (W200P, Campbell Scientific Ltd, UK) located 8.5 m high on a mast situated 3 m over the greenhouse ridge (A 100R. Campbell Scientific Ltd, UK).
- The outside global radiation Rgo was measured by means a pyranometer (SP-LITE, Kipp & Zonen, Campbell Scientific Ltd, UK).

The parameters described in Table 1 were systematically recorded, in order to determine the simulation boundary conditions and to validate the simulation model.

RESULTS AND DISCUSSIONS

After validation of our model (Majdoubi, 2007) details of air wind speed, temperature and specific humidity patterns in vertical or longitudinal profiles of the three studies cases: i) the 4 sidewall closed (TPF), ii) the north and south sidewall closed (PNSF) and iii) the 4 sidewall opened (TPO), were presented in figures 3 to 13.

i. Airflow circulation

For an outside wind direction perpendicular to the roof ventilation openings (i.e. west-east). Figure 3, illustrates a vertical cross-section along the flow direction in the middle of the greenhouse for the three configurations. It shows the development, at the level of crop cover, of a reverse flow from the leeward end to windward end part of the greenhouse for the three studies configurations, the wind speed at this level being much lower than above vegetation. However, it is noted that, with a north-south side wall ventilation opening closed, the velocity above the canopy is greater than for the other configurations. Velocity profiles are similar in the case where the sidewall ventilation openings are fully closed or open, either in or above the vegetation.

It therefore appears that, paradoxically, the closure of the North-South sidewall ventilation openings contributes significantly to increase the air exchange in the greenhouse, the roof ventilation opening also contributing significantly. The air velocity profiles across the middle of the greenhouse at heights of 1, 3 and 4 m were reported in Figures 4, 5 and 6. Results confirm the results of the previous figure concerning the airflow. The velocities in the vegetation at 1m above the soil surface are low in all three cases, with however a slight increase of wind speed in the case where the north and south sidewalls ventilation opening are closed. At the level of 3 m and 4 m above soil area, we also note that with a north and south sidewalls ventilation openings closed, the wind speed is highest in the greenhouse. Consequently, we can conclude that the contribution of the west sidewall ventilation opening, limited of an effect in the first 30 meters from the windward of the ventilation opening. After these are the roof ventilation openings which feed the air circulation in the greenhouse.

These results confirm that greenhouse air velocity is governed mainly by roof ventilation openings at the gutter and it appears clearly that the roof openings are alternatively acted as air entrances and exits, which confirm the results observed by Majdoubi et al., 2009.

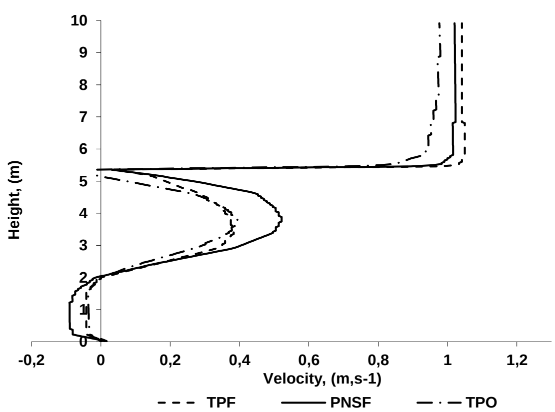

Figure 3. Modeled profile of mean horizontal wind speed in the center of the greenhouse with three different vent configurations.

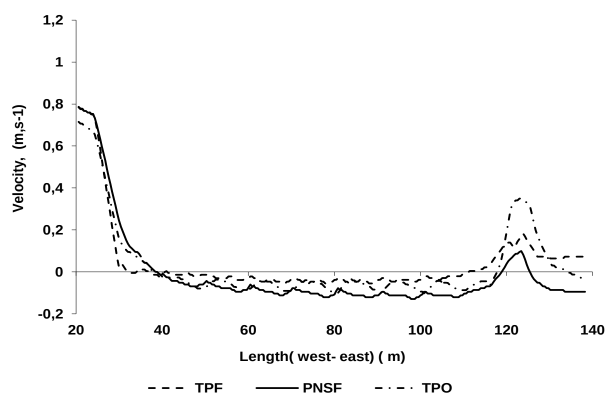

Figure 4. Modeled horizontal air velocity profiles across the middle of the greenhouse along West–East direction at height 1m above soil surface.

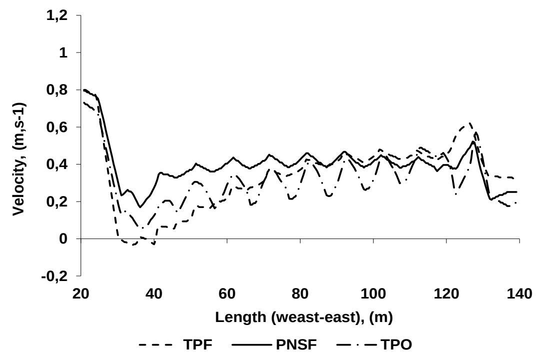

Figure 5. Modeled horizontal air velocity profiles across the middle of the greenhouse along West–East direction at height 3m above soil surface.

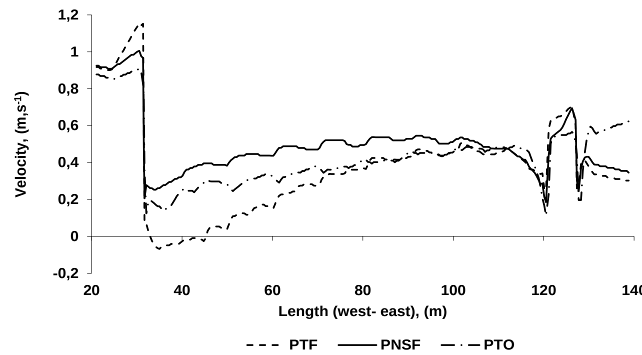

Figure 6. Modeled horizontal air velocity profiles across the middle of the greenhouse along West–East direction at height 4m above soil surface.

Figures 7 and 8 illustrate the horizontal velocity profiles respectively at 1 and 4 m above the ground (from north to south). Results show that the north opening and south one contribute mainly to increase in the air wind speed only near the sides (up to 4 m), for the profile practiced at 1 m above the ground.

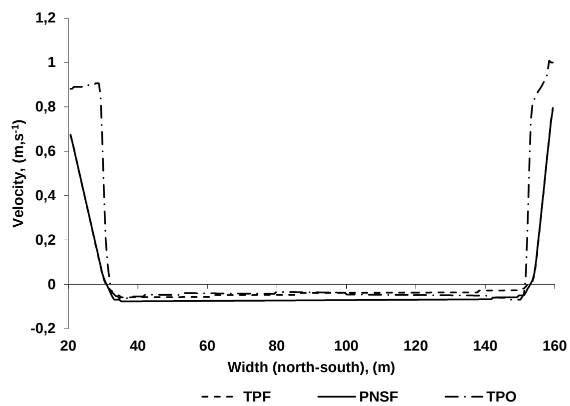

Figure 7. Modeled horizontal air velocity profiles across the middle of the greenhouse along North-South direction at height 1m above soil surface.

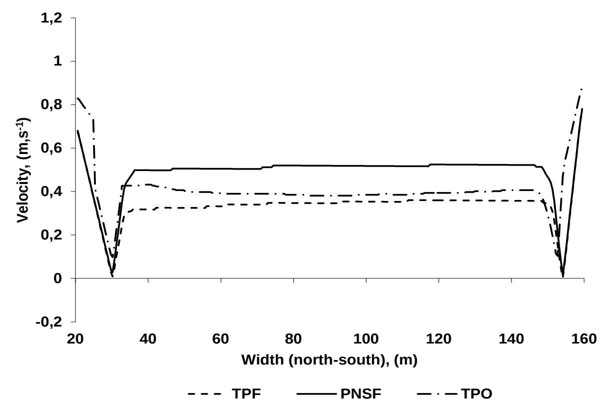

Figure 8. Modeled horizontal air velocity profiles across the middle of the greenhouse along North-South direction at height 4m above soil surface.

ii. Temperature and humidity patterns

Figures 9 and 10 illustrate respectively the vertical profiles of simulated air temperature and specific humidity in the center of the greenhouse respect to the height. We can observe through the previous figures that there is no significant difference of air temperature and specific humidity between the three cases except at the soil surface where it is found that the temperature and specific humidity were higher (by about respectively 0.5° C and 5.66 10^{-5}) in the case where the four sidewalls ventilation openings ware open.

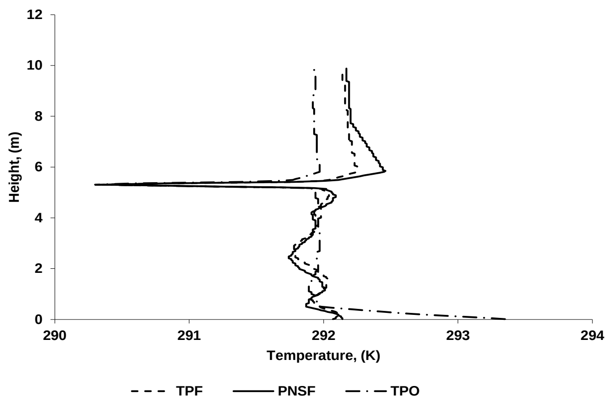

Figure 9. Modeled vertical profile of air temperature in the centre of the greenhouse between two successive roof openings.

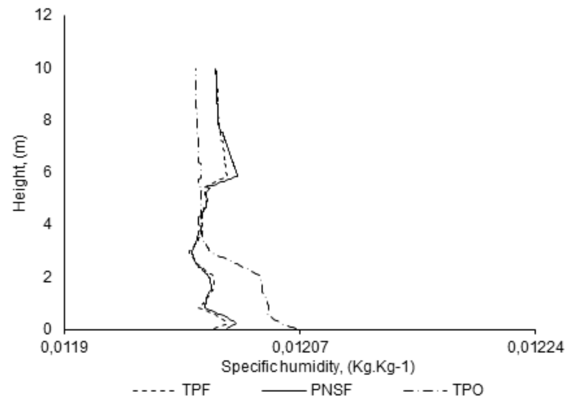

Figure 10. Modeled vertical profile of air specific humidity in the centre of the greenhouse between two successive roof openings.

Figures 11 and 12 show the air temperature and specific humidity profiles respectively along the length of the greenhouse at 1m above the ground. It is clear that the closing or opening of the sidewalls has no significant effect on canary greenhouse air temperature during the nighttime, but we can observe a slight increase of specific humidity for the case with all side wall ventilation openings were open.

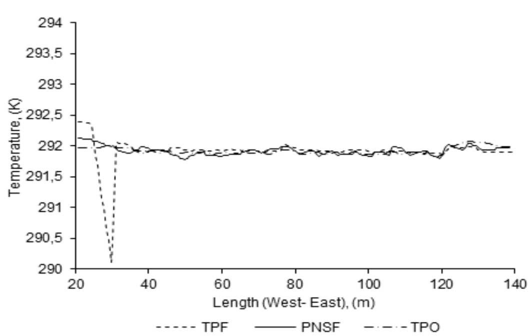

Figure 11. Modeled horizontal profiles of air temperature in the centre of the greenhouse from the West to the East at 1m high above soil surface.

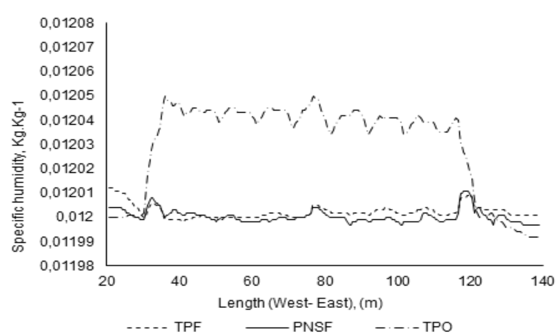

Figure 12. Modeled horizontal profiles of air specific humidity in the centre of the greenhouse from the West to the East at 1m high above soil surface.

The horizontal profiles of air temperature and specific humidity respectively at 1m above the ground as a function of the width of the greenhouse (from north to south) were plotted in figure

12 and 13, we can observe that temperature and specific humidity values are the same for all configurations and that the climate is homogeneous at the same height.

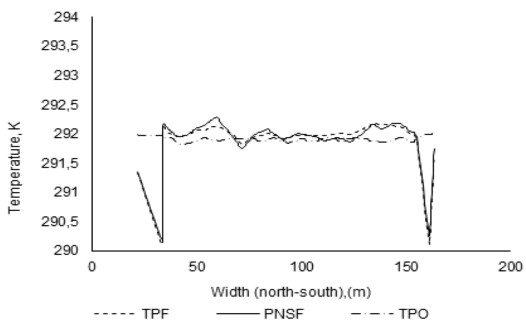

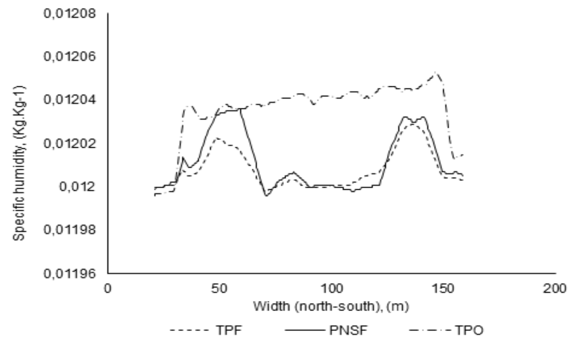

Figure 13. Modeled horizontal air temperature profiles across the middle of the greenhouse along North-South direction at height 1m above soil surface.

Figure 14. Modelled horizontal air specific humidity profiles across the middle of the greenhouse along North-South direction at height 1m above soil surface.

CONCLUSION

A 3D numerical simulation model of large scale canary greenhouse was developed and validated. Based on our results for the three vents opening configurations studied (the 4 side wall vents opening closed, the north-south side wall vents opening closed and the 4 side wall vents opening opened), it appears that during night time there is no significant effect of side wall vents opening on canary greenhouse wind speed, temperature and humidity values compared with the outside climate. So, we can make the following points:

The opening of the forth greenhouse sidewall is not the configuration which can allows a maximum air exchange and therefore the moisture management related to the transpiration of the crop.

The closure of the forth is accompanied by a limitation of the greenhouse air velocity, and thus renewed, but curiously does not induce increase moisture in the vegetation. This is paradoxical but is not very well explained.

The opening only of the side wall located upwind and downwind accelerates the greenhouse air circulation which thus enables to remove excess moisture generated by perspiration of culture.

REFERENCES

Boulard, T., & Baille, A. (1995). Modelling of air exchange rate in a greenhouse equipped with continuous roof vents. *Journal of Agricultural Engineering Research*, 61, 37-48.

Boulard, T., & Draoui, B. (1995). Natural ventilation of a greenhouse with continuous roof vents: measurements and data analysis. *Journal of Agricultural Engineering Research*, 61, 27-36.

Boulard, T., Baille, A., Mermier, M., & Villette, F. (1991). Mesures et modélisation de la résistance stomatique foliaire et de la transpiration d'un couvert de tomates de serre. (Measurement and modeling of tomato leaf stomatal resistance and transpiration in greenhouse conditions). *Agronomie*, 11(4), 259–274.

Bruse M. (1998). Development of a numerical model for the simulation of exchange processes between small scale environmental design and microclimate in urban areas. Ph.D. Thesis. University of Bochum.

Campen, J. B., & Bot, G. P. A. (2003). Determination of greenhouse-specific aspects of ventilation using three-dimensional computational fluid dynamics. *Biosystems Engineering*, 84(1), 69-77.

Demrati, H., Boulard, T., Fatnassi, H., Bekkaoui A., Majdoubi H., Elattir H., & Bouirden L. (2007). Microclimate and transpiration of a greenhouse banana crop. *Biosystems Engineering*, 98, 66-78.

Fatnassi, H., Leyronas, C., Boulard, T., Bardin, M., & Nicot, P. (2009). Dependence of greenhouse tunnel ventilation on wind direction and crop height. *Biosystems Engineering*, 103(3):338-343.

Fatnassi, H., Boulard, T., & Bouirden, L. (2003). Simulation of climatic conditions in full scale greenhouse fitted with insect proof screens. *Agricultural and Forest Meteorology*, 118, 97-111.

Fatnassi, H., Boulard, T., Poncet, C., & Chave, M. (2006). Optimisation of greenhouse insecte screening with Computational Fluid Dynamics. *Biosystems Engineering*, 93(3), 301- 312.

Feuilloley, P., Mekikdjian, C., & Lagier, J. (1994). Natural ventilation of plastic tunnel greenhouses in the Mediterranean. *Plasticulture*, 104, 33−46.

Majdoubi, H., Boulard, T., Fatnassi, H., & Bouirden, L. (2009) Airflow and microclimate patterns in a one-hectare Canary type greenhouse: An experimental and CFD assisted study. *Agricultural and Forest Meteorology*, 149, 1050–1062.

Haxaire, R. (1999). Caractérisation et Modélisation des écoulements d'air dans une serre (Characterization and Modeling of air flows in a greenhouse). Ph.D. Thesis de l'Université de Nice, Sophia Antipolis., 148p.

Issa, R. I. (1985). Solution of the implicity discritized fluid flow equations by operator-splitting. *Journal of computational Physics*, 62, 40-65.

Kittas, C., Boulard. T., Mermier, M., & Papadakis, G. (1996). Wind induced air exchange rates in a greenhouse tunnel with continuous side openings. *Journal of Agricultural Engineering Research*, 65, 37-49.

Kittas, C., Draoui, B., & Boulard, T. (1995). Quantification of the ventilation rate of a greenhouse with a continuous roof opening. *Agricultural and Forest Meteorology*, 77, 95-111.

Launder, B. E., & Spalding, D. B. (1974). The numerical computational of Turbulent flows. *Computer Methods in Applied Mechanics and Engineering*, 3, 269-289

Majdoubi, H., Boulard, T., Hanafi, A., Bekkaoui, A., Demrati, H., Fatnassi, H., Nya, M., & Bouirden, L. (2007). Natural ventilation performance of a large scale canary greenhouse equipped with insect screens. *Transections of ASAE*, 50(2), 641−650.

Majdoubi, H. (2007). Contribution à la modélisation du microclimat des serres. PhD Thesis, Université Ibn Zohr, Faculté des Sciences d'Agadir, No D55/2007, 215pp.

Miguel, A. F., Van den Break, N. J., Bot, G. P. A. (1997). Analysis of the airflow characteristics of greenhouse screening materials. *Journal of Agricultural Engineering Research*, 67, 105-112.

Molina-Aiz, F. D., Valera, D. L., & Alvarez, A. J. (2004). Measurement and simulation of climate inside Almeria-type greenhouses using computational fluid dynamics. *Agricultural and Forest Meteorology*, 125, 33-51.

Patankar, S. V. (1980). Numerical heat transfer and fluid flow. Hemisphere, New York.

Piscia, D., Muñoz, P., Panadès, C., & Montero, J. I. (2015). A method of coupling CFD and energy balance simulations to study humidity control in unheated greenhouses. *Computers and Electronics in Agriculture*, 115, 129–141.

Sase, S. (2006). Air movement and climate uniformity in ventilated greenhouses. *Acta Horticulturae (ISHS)*, 719, 313-324.

Willits, D. H., Li, S., & Yunker, C. A. (2006). The cooling performance of naturally ventilated greenhouses in the southeastern U.S. *Acta Horticulturae (ISHS)*, 719, 73-82.